

Settlement and additional internal forces of grouped piles in layered soil

G. MYLONAKIS* and G. GAZETAS†

This paper recognizes that soil layering may have a profound effect on the settlement of pile groups and that pile-to-pile interaction induces not only additional settlement at the head of each pile but also additional stresses along its shaft. A general analytical formulation is developed, based on the Winkler model of soil reaction, for determining the vertical interaction factors between two piles embedded in multi-layered soil. It is shown that such interaction factors depend not only on the displacement field arising from the settlement of a loaded ('source') pile but also on the interplay between the adjacent ('receiver') pile and the soil subjected to this displacement field. Such interplay, which has not been considered (at least explicitly) in currently available simple methods, is quantified here through an analytically determined factor ζ , which lies between 0 and 1. The paper also develops closed-form expressions for pile stiffness and interaction factors in a two-layer stratum, and highlights crucial aspects of the problem.

KEYWORDS: numerical modelling and analysis; piles; settlement; soil/structure interaction; stiffness.

L'article reconnaît que la stratification du sol peut avoir de profonds effets sur le tassement des groupes de pieux et que l'interaction entre les pieux produit non seulement un tassement supplémentaire à la tête de chaque pieu, mais aussi des contraintes supplémentaires le long de son fût. Les auteurs ont mis au point une formule analytique générale basée sur le modèle de réaction du sol de Winkler pour déterminer les facteurs d'interaction verticale entre deux pieux enfoncés dans un sol à couches multiples. Ils montrent que ces facteurs dépendent non seulement du champ de déplacement engendré par le tassement d'un pieu chargé («source»), mais aussi de l'interaction entre le pieu adjacent («récepteur») et le sol soumis à ce champ de déplacement. Cette interaction, dont ne tiennent pas compte (du moins explicitement) les méthodes simples actuellement disponibles, est quantifiée ici à l'aide d'un coefficient ξ établi par analyse, qui se situe entre 0 et 1. L'article présente également des expressions de forme fermée pour la rigidité des pieux et les coefficients d'interaction dans un sol à deux couches, et fait ressortir les principaux aspects du problème.

INTRODUCTION

A number of rigorous numerical techniques such as the boundary-element-type methods (Poulos, 1968; Butterfield & Banerjee, 1971; Banerjee & Davies, 1978) and the finite element method (Ottaviani, 1975) have been used for pile settlement analysis. However, a number of approximate solutions, based on sound principles of mechanics (Cooke, 1974; Randolph & Wroth, 1978, 1979; Baguein & Frank, 1979; Scott, 1981; Nogami & Chen, 1984; Chow, 1986; Fleming *et al.*, 1992), have provided valuable insight and offered versatile design methods. A comprehensive review of the

subject was presented in the Rankine lecture by Poulos (1989).

The simplified (yet rational) concept of *interaction factors* was introduced by Poulos in 1968, who showed that pile group effects can be assessed by superimposing the effects of only two piles at a time. Numerous subsequent studies have shown that pile-to-pile interaction (PPI) (*a*) leads to a decrease in the group stiffness, (*b*) distributes non-uniformly the cap load with the corner piles 'attracting' more load than the central piles, and (*c*) alters the load-transfer mechanism by producing additional shear stresses along the pile shaft and increasing the load transmitted to the base. However, despite the fact that the latter effect has been clearly pointed out in some studies (Poulos, 1968; Ghosh, 1975; Ottaviani, 1975), there is currently almost no information on its importance, and certainly no simple method available to compute it.

Manuscript received 3 January 1996; revised manuscript accepted 11 November 1996.

Discussion on this paper closes 1 May 1998; for further details see p. ii.

* City College of City University of New York.

† National Technical University, Athens.

The scope of this paper is twofold: (a) to develop a simple and effective procedure for calculating multilayer interaction factors and to apply it in pile-group settlement analysis, and (b) to investigate quantitatively the effect of pile-to-pile interaction on the mechanism of transferring cap load to the soil mass through the piles.

PROBLEM DEFINITION

The general system studied in this paper consists of a group of m vertical compressible piles embedded in a layered soil deposit (Fig. 1(a)). The system is subjected to a vertical static load P_G transmitted through a rigid pile cap which has no contact with the soil. Each soil layer is modelled as a linear elastic material of Young's modulus E_s and Poisson's ratio ν_s . Although the method is also applicable to groups containing piles of different sizes and properties, in this paper all piles are considered to be identical solid cylinders of length L , diameter d , cross-sectional area A_p and Young's modulus E_p . The (usually stiffer) soil below the pile tip extends either to infinity (half-space) or terminates at bedrock, located at a depth h_b from the pile tip. The pile spacing is denoted by s and the thickness of the i th soil layer by h_i . No slippage is allowed to occur at the pile-soil interface. The sign convention in this paper is illustrated in Fig. 1(b).

This system is analysed in three consecutive steps: (1) behaviour of a single pile, (2) pile-to-pile interaction and (3) settlement and internal forces of the grouped piles.

THE SINGLE PILE

From the simple method of Randolph & Wroth (1978) it follows that the soil around a pile shaft can be represented by distributed springs (Winkler assumption), the stiffness of which (per unit length of pile) can be written as

$$k_z = \delta G_s \quad (1a)$$

where

$$\delta = \frac{2\pi}{\ln\left(\frac{2r_m}{d}\right)} \quad (1b)$$

and r_m is a 'magical' (in the words of Randolph & Wroth) radius, beyond which soil settlement is vanishingly small. In the general case of an inhomogeneous soil, r_m is given by

$$r_m \approx \chi_1 \chi_2 L (1 - \nu_s) \quad (2)$$

in which χ_1 and χ_2 are empirical factors accounting for soil inhomogeneity; their numerical values are discussed later in this paper.

Pile base

Adopting the arguments of Randolph & Wroth (1978) and Scott (1981), it is sufficient to assume that the pile base ('tip') acts as rigid circular disc on the surface of a homogeneous elastic stratum. The corresponding force-displacement relationship can be written as follows:

$$K_b \equiv \frac{P_b}{W_b} \approx \frac{dE_b}{1 - \nu_b^2} \left(1 + 0.65 \frac{d}{h_b}\right) \quad (3)$$

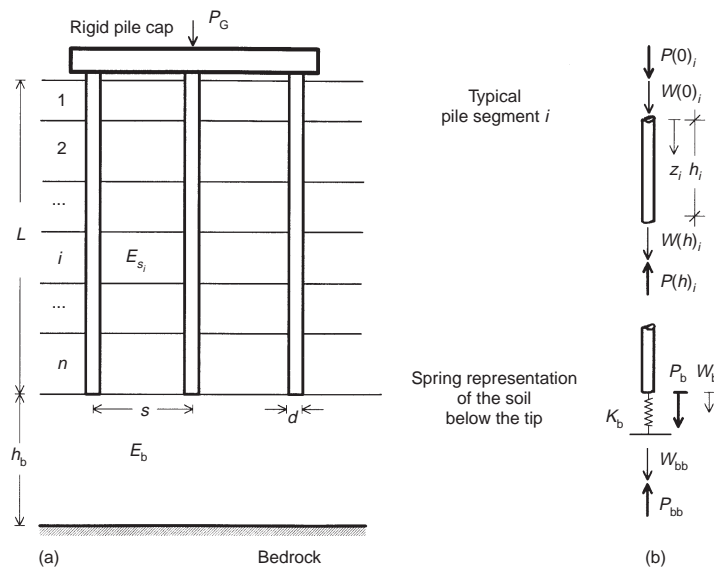


Fig. 1. (a) Problem studied in this paper; (b) sign convention

The factor in parentheses on the right-hand side of equation (3) accounts for the presence of a rigid bedrock at depth equal to h_b below the pile tip (Kausel, 1974; Gazetas, 1983); evidently, with no bedrock present, $h_b \rightarrow \infty$ and this term reduces to unity.

In the case of a pile in a homogenous layer, the solution of the governing equilibrium equation yields the vertical stiffness K atop the pile:

$$K = E_p A_p \lambda \frac{\Omega + \tanh(h\lambda)}{1 + \Omega \tanh(h\lambda)} \quad (4a)$$

in which Ω and λ stand for the dimensionless pile-base stiffness and load transfer (Winkler) parameter respectively:

$$\Omega \equiv \frac{K_b}{E_p A_p \lambda} \quad (4b)$$

$$\lambda \equiv \sqrt{\left(\frac{\delta G_s}{E_p A_p}\right)} \quad (4c)$$

(In single-layer soils, the pile length L is equal to the layer thickness h . In this case we use h instead of L .)

Equation (4a) is portrayed parametrically in Fig. 2 in terms of the dimensionless pile length $h\lambda$. The pile stiffness is normalized by the stiffness of an infinitely long pile, $E_p A_p \lambda$, and is plotted for five

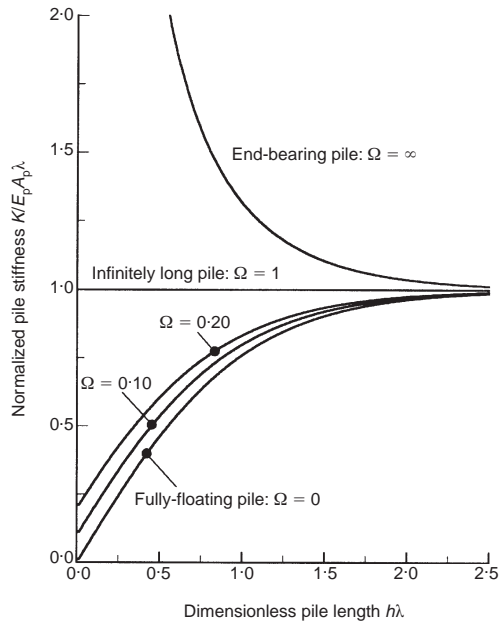


Fig. 2. Normalized stiffness of a compressible pile embedded in single-layer soil, for different values of the dimensionless base stiffness Ω

different stiffness values Ω . Several interesting trends are worthy of note in this figure.

- (a) For the limiting case of $\Omega = 0$ (no soil reaction at the pile tip), the stiffness of a fully floating pile grows linearly with $h\lambda$ up to a value of $h\lambda \approx 0.50$. This implies that within the range $0 < h\lambda < 0.50$, a fully floating pile is essentially rigid. For $h\lambda > 0.50$, the pile gradually becomes more compressible and pile stiffness increases at a slower rate, reaching 90% of the stiffness of the infinitely long pile at $h\lambda \approx 1.50$. This value defines an *active length* beyond which pile stiffness does not increase with pile length. Substituting $h\lambda = 1.50$ into equation (4c) leads to

$$(L/d)_{\text{active}} \approx 1.75(E_p/E_s)^{1/2} \quad (5)$$

This expression is similar to the one reported by Poulos (1989), and for $E_p/E_s = 1000$ gives an active length at the order of 60 pile diameters—well above most pile lengths used in practice. Therefore, contrary to laterally loaded piles, for which the active length is usually of the order of 10 diameters, in axially loaded piles active length is too large to be of practical significance.

- (b) Similar trends are observed for floating piles with $\Omega = 0.10$ and 0.20 . Specifically, the normalized pile stiffness (i) tends to become equal to Ω as the pile length tends to zero (i.e. the stiffness of a zero-length pile is equal to the stiffness of the soil ‘spring’ at the pile tip), (ii) increases almost linearly with $h\lambda$ up to $h\lambda \approx 0.50$, and (iii) reaches its limiting (asymptotic) value at $h\lambda$ about 1.75, regardless of Ω .
- (c) A different behaviour characterizes end-bearing piles. Their stiffness is a monotonically decreasing function of pile length. It is easy to prove from equation (4a) that the product of the stiffness of an end-bearing pile ($\Omega = \infty$) and the stiffness of a fully floating pile ($\Omega = 0$) of the same length is equal to the square of the stiffness of the infinitely long pile. This remarkable property is apparent in Fig. 2, showing that the curve $\Omega = 1$ is the geometric mean of the curves for $\Omega = \infty$ and $\Omega = 0$.

For a pile embedded in a two-layer soil, a closed-form expression is obtained for the stiffness of the pile (see derivation in Appendix 1):

$$K = E_p A_p \lambda_1 \frac{\lambda_1 \tanh(h_1 \lambda_1) + \lambda_1 \Omega \tanh(h_1 \lambda_1) \tanh(h_2 \lambda_2) + \lambda_2 \Omega + \lambda_2 \tanh(h_2 \lambda_2)}{\lambda_1 + \lambda_1 \Omega \tanh(h_2 \lambda_2) + \lambda_2 \Omega \tanh(h_1 \lambda_1) + \lambda_2 \tanh(h_1 \lambda_1) \tanh(h_2 \lambda_2)} \quad (6)$$

The reader can easily verify that by setting $h_1 = 0$, equation (6) reduces to the single-layer equation (4a).

The numerical values of χ_1 and χ_2 are discussed by Randolph & Wroth (1978). They recommend $\chi_1 = 2.5$ for piles in a half-space and $\chi_1 = 2.0$ for soil on rigid bedrock at depth $2.5L$. Also, for a homogeneous half-space χ_2 is about 1.0, whereas for 'Gibson'-type soil χ_2 is about 0.5. Clearly, judgement is necessary to interpolate the above empirical values for an intermediate multilayer soil. Fortunately, however, the single-pile stiffness is insensitive to the 'exact' value of magical radius r_m . As an example, we consider a pile of slenderness ratio $L/d = 30$ embedded in multilayer soil having an average Poisson's ratio $\nu_s = 0.3$. For a particular soil layer, the Winkler parameter λ is calculated assuming that

- (a) $\chi_1\chi_2 \approx 2.5$ (i.e. homogeneous half-space conditions)
 (b) $\chi_1\chi_2 \approx 1.0$ (i.e. Gibson soil on bedrock conditions).

Despite the huge discrepancy in magical radius (by a factor of 2.5), the two choices yield very similar Winkler parameters:

$$\frac{\lambda^{(a)}}{\lambda^{(b)}} = \sqrt{\left(\frac{\ln[2 \times 1.0 \times 30(1 - 0.3)]}{\ln[2 \times 2.5 \times 30(1 - 0.3)]}\right)} \approx 0.90 \quad (7)$$

Moreover, recalling that, for floating piles, the stiffness increases with λ by a less-than-linear rate (see Fig. 2), the resulting difference in pile stiffness is even smaller (less than 6%)—a negligible difference compared with the many uncertainties in real-life problems. Therefore, for single piles, reasonable estimates of settlement can be achieved by selecting χ_1 and χ_2 equal to either the homogeneous half-space values, 2.5 and 1.0, or the Gibson soil on rock values, 2.0 and 0.50. Additional discussion on χ_1 and χ_2 is given in the sequel.

Further justification of the validity of the above argument comes from Fig. 3, where the predictions of equation (6), using the 'homogeneous half-space' values $\chi_1 = 2.5$ and $\chi_2 = 1.0$, are contrasted with the results of Poulos & Davis (1980) and Valliappan *et al.* (1974), for an incompressible pile of length L embedded in a two-layer soil deposit (the thickness of the top layer is $h_1 < L$, the bottom layer is a half-space and the Young's moduli E_{s1} and E_{s2} have a ratio ranging from 0.2 to 5). The comparison between the expression developed here and Poulos' approximate numerical solution is very good for the whole range of h_1/L values. The same good comparison is noted against the finite element results of Valliappan *et al.* (1974).

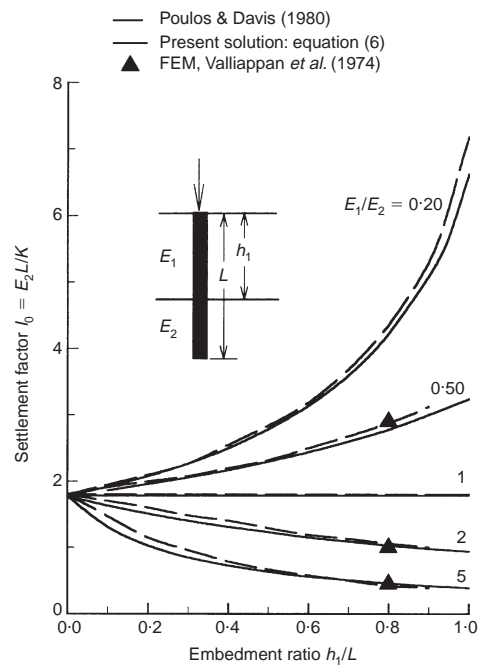


Fig. 3. Comparison of the closed-form expression developed here (equation (6)) for the pile stiffness in a two-layer soil with results from numerical solutions ($\chi_1 = 2.5$, $\chi_2 = 1$)

INTERACTION BETWEEN TWO PILES

To determine the interaction factor between two piles, one may start by calculating the displacement field around a single loaded ('source') pile. The plane-strain approximation yields a logarithmic variation of vertical soil displacement U_s with radial distance s from the pile and thereby to an *attenuation function* expressed as

$$\psi(s) \equiv \frac{U_s(s, z)}{U_s(d/2, z)} = \begin{cases} \frac{\ln(r_m) - \ln(s)}{\ln(2r_m) - \ln(d)} & \frac{d}{2} < s < r_m \\ 0 & s \geq r_m \end{cases} \quad (8)$$

Naturally, this plane-strain function $\psi(s)$ is independent of the depth z .

Assuming that (i) the pile is stiff compared with the surrounding soil (i.e. the gradient of pile settlement with depth is relatively small) and (ii) a second, unloaded pile (hereafter called the 'receiver' pile) located at a distance s from the 'source' pile follows exactly the free-field soil displacement described in equation (8), the interaction factor would be (approximately) equal to $\psi(s)$. This is

essentially what Randolph & Wroth (1979) assumed for calculating pile shaft-to-shaft interaction.

A new model for pile-to-pile interaction

In reality, however, piles do not follow exactly the free-field displacement generated by their neighbours. Axial pile rigidity and the soil reaction at the pile tip tend to reduce the settlement from the value computed on the basis of equation (8)—hence the need for a more refined model, especially for piles in multilayered soil.

To this end, we propose a method involving three consecutive steps, illustrated in Fig. 4.

Step 1. The ‘source’ pile is subjected to a vertical load at its head. Applying the method given in Appendix 1 (or any other analytical approach), the settlement profile $W_{11}(z)$ along the pile is determined.

Step 2. For a soil profile consisting of distinct, homogeneous horizontal layers it is assumed that the attenuation of soil settlement with radial distance from the pile still obeys (even if only approximately) the logarithmic variation of equation (8), within each layer. Therefore, at the location of the unloaded ‘receiver’ pile, if this pile were not present, the soil displacement would be

$$U_s(s, z) \approx W_{11}(z)\psi(s) \tag{9}$$

Step 3. The presence of the ‘receiver’ pile modifies (usually reduces) the above displacement. To account in a simple yet realistic way for the interplay between receiver pile and soil, the receiver pile is modelled as a beam supported with Winkler springs. Loading originates as a support movement, equal to the attenuated vertical displacement field $U_s(s, z)$ of Step 2. (An analogous model was used by Makris & Gazetas (1992) to study the lateral dynamic interaction of piles.) The mechanics of this loading is in a sense the reverse of that of Step 1, in which the source pile induces displacements in the soil; in Step 3, the soil induces the (attenuated) displacements on the source pile. The response of the receiver pile, $W_{21}(z)$, to such indirect loading leads to the interaction factor, defined as

$$\alpha = \frac{W_{21}(z=0)}{W_{11}(z=0)} \tag{10}$$

For this last Step 3, the analysis begins with setting up the governing differential equation for each soil layer. With the spring reaction being proportional to the relative displacement $W_{21}(z) - U_s(z)$, vertical equilibrium of an element of the receiver pile is written as

$$E_p A_p \frac{d^2 W_{21}(z)}{dz^2} - k_z [W_{21}(z) - U_s(s, z)] = 0 \tag{11a}$$

where U_s has been obtained, for each soil layer, from Steps 1 and 2:

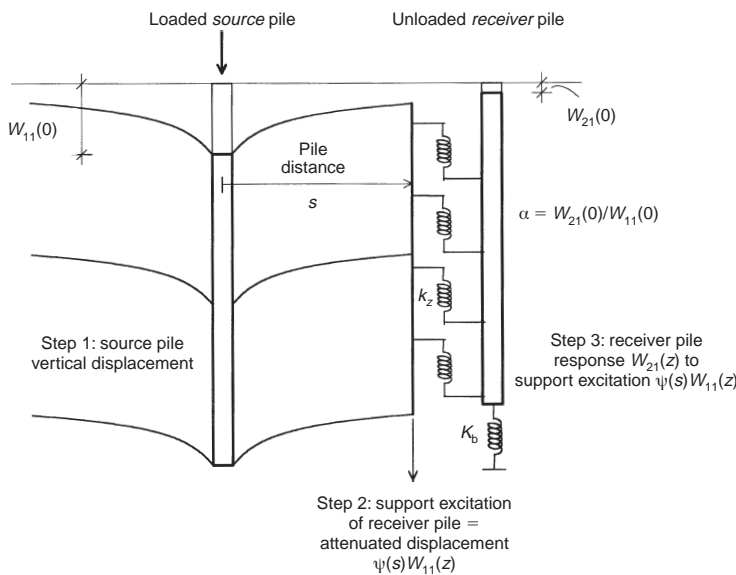


Fig. 4. Schematic illustration of the proposed model for computing the influence of a head-loaded ‘source’ pile on the adjacent (unloaded) ‘receiver’ pile, in a layered soil

$$U_s(s, z) = \psi(s)W_{11}(z) = \psi(s)(A_{11}e^{\lambda z} + B_{11}e^{-\lambda z}) \quad (11b)$$

A_{11} and B_{11} are integration constants determined from the boundary conditions of the *source* pile. The solution to equation (11a) is

$$W_{21}(z) = \frac{\lambda}{2}\psi(s)z[-A_{11}e^{\lambda z} + B_{11}e^{-\lambda z}] + A_{21}e^{\lambda z} + B_{21}e^{-\lambda z} \quad (12)$$

(It is of interest that the two exponentials in the forcing term of equation (11) coincide with the homogeneous solution of that equation. As a result, the independent variable z has to be included in the particular integral to ensure the independence between the homogeneous and particular solutions (see Sokolnikoff & Redheffer, 1966).) A_{21} and B_{21} are new integration constants to be determined from the boundary conditions of the *receiver* pile (i.e. zero force atop the pile, continuity of forces and displacements at each layer interface and at the tip). The general formulation for n soil layers involves matrix algebra which is quite standard. Elements of such an analysis are given in the sequel. More details can be found in the doctoral thesis of Mylonakis (1995).

As an example, in the particular case of a pile in a single-layer soil, equation (12) yields an explicit expression for the interaction factor a , as a product of two functions:

$$a = \psi(s)\zeta(h\lambda, \Omega) \quad (13a)$$

where the function $\zeta = \zeta(h\lambda, \Omega)$ is given by

$$\zeta = \frac{2h\lambda + \sinh(2h\lambda) + \Omega^2[\sinh(2h\lambda) - 2h\lambda] + 2\Omega[\cosh(2h\lambda) - 1]}{2\sinh(2h\lambda) + 2\Omega^2\sinh(2h\lambda) + 4\Omega\cosh(2h\lambda)} \quad (13b)$$

Of these two functions, ψ denotes the induced free-field displacement, while ζ represents the effect of the rigidity of the pile and the interaction between the pile and surrounding soil. Recall that Randolph & Wroth (1979) assumed that the shaft of the receiver pile follows exactly the induced free-field soil settlement generated at mid-depth of the source pile (i.e. they neglected Step 3 and assumed $\zeta = 1$). Chow (1986) divided the profile into discrete horizontal soil layers (in a similar manner as was done here) but he also implicitly assumed, as did Randolph & Wroth, that within a soil layer, the settlement of a pile segment j due to pile segment i is given by the free-field equation (8). As a result, for homogeneous soil, his solution is essentially the same as that of Randolph & Wroth (1979).

It is instructive to examine the asymptotic behaviour of the function $\zeta = \zeta(h\lambda, \Omega)$ (equation

(13b)). For end-bearing piles, the base-stiffness parameter Ω becomes infinite and ζ simplifies to

$$\zeta = \frac{1}{2}\left[1 - \frac{2h\lambda}{\sinh(2h\lambda)}\right] \quad (14)$$

whereas for *base-unsupported*, fully-floating piles, the base parameter Ω vanishes and

$$\zeta = \frac{1}{2}\left[1 + \frac{2h\lambda}{\sinh(2h\lambda)}\right] \quad (15)$$

For a very long pile, as h approaches infinity, all the above equations converge to

$$\zeta = \frac{1}{2} \quad (16)$$

This remarkable outcome implies that with very long piles, the interaction factor is only one-half of the 'free-field' value at the location of the receiver pile. Also, notice that equation (16) is equal to one-half of the sum of equations (14) and (15) (i.e. the interaction factor of a fully floating pile is symmetric to that of the end-bearing pile with respect to the infinitely long pile); further discussion is given in the sequel.

Interaction between pile bases

The analysis presented so far considers only the interaction between pile shafts. However, a displacement field is also generated below a pile base. As a result, interaction will also develop between pile bases. Its importance is examined here.

Following the assumption that the pile base acts as a punch on the surface of a half-space, the attenuation of soil settlement at a radial distance s from the pile is given by

$$\psi_b(s) \equiv \frac{U_s(s, L)}{U_s(d/2, L)} \approx \frac{d}{\pi s} \quad (17)$$

This approximation has been found by Randolph & Wroth (1979) to be in accord with the 'exact' settlement profile around a rigid punch on a half-space, for $s > d$.

Interaction between pile bases can be included in the proposed method by simply assuming that the attenuated settlement $\psi_b(s)W_b$ generated from the load P_b at the base of the source pile drags downwards the *base* of the spring at the tip of the receiver pile.* Enforcing this new boundary condition, a complementary interaction factor a_b is calculated, accounting for pile base-to-base inter-

* The spring at the pile tip is a stiffness element having, of course, no dimensions (i.e. length) and therefore base-to-base interaction, as treated in this paper, occurs at the same elevation.

action. As an example, in the case of a homogeneous single-layer soil, a_b can again be expressed explicitly as the product of two functions:

$$a_b = \psi_b(s)\zeta_b(h\lambda, \Omega) \quad (18a)$$

where the function $\zeta_b = \zeta_b(h\lambda, \Omega)$ is given explicitly as (Mylonakis, 1995)

$$\zeta_b = \frac{2\Omega}{2\Omega \cosh(2h\lambda) + \sinh(2h\lambda)(\Omega^2 + 1)} \quad (18b)$$

Using the arguments of Randolph & Wroth (1978), the overall interaction factor is approximately equal to the sum of the shaft-to-shaft component a and the base-to-base component a_b .

The major difference between shaft and base attenuation functions is that $\psi_b(s)$ decreases in inverse proportion to the radial distance s , while $\psi(s)$ decreases at a much slower (logarithmic or square-root) rate. Therefore, base displacement affects a substantially smaller region around a pile than shaft displacement. (For example, for $s/d = 2$, ψ_b is equal to only 0.13—about 4 times smaller than ψ ; for $s/d = 4$, ψ_b is equal to 0.08 or about 5 times smaller than ψ .) Moreover, soil–base interaction further reduces a_b . To illustrate this, Fig. 5 plots ζ_b versus $h\lambda$ and Ω . It is seen that ζ decreases very fast with pile length, remaining below 0.20 for most cases of practical interest. Evidently, a_b (the product of two small numbers) would be much smaller than unity (usually of the

order of 10^{-3}). Therefore, pile base-to-base interaction is negligible and will not be further addressed in this paper.

Returning to (the dominant) shaft-to-shaft interaction, the function $\zeta = \alpha/\psi(s)$ (equation (13b)) is plotted in Fig. 6 as a function of the dimensionless pile length $h\lambda$. Expressing solely pile–soil interaction, ζ is always less than 1. For zero pile length, ζ vanishes since a source pile of zero length cannot produce any appreciable ‘action’ (i.e. displacement field) to affect its neighbours (interaction between pile bases has already been neglected). The only exception to this is the zero-length fully floating pile; having zero stiffness, it follows exactly the (vanishingly small) action by the source pile, leading to $\zeta = 1$.

For values of Ω between 0 and 1, several trends are noted: initially, for short piles, ζ increases rapidly with pile length $h\lambda$, reaching a peak at $h\lambda$ of the order of 0.50; thereafter, for long piles, ζ turns to a decreasing function of $h\lambda$ approaching asymptotically the value of 0.50. Notice that the peaks occur at a value of $h\lambda$ which increases with Ω . A qualitative explanation of these trends is offered below.

The initial increasing trend is a result of the essentially rigid behaviour of short piles. Indeed, the equilibrium of a rigid receiver pile embedded in a single-layer soil leads to

$$\int_0^h k_z[\alpha - \psi(s)] dz + \int_0^h dP = 0 \quad (19a)$$

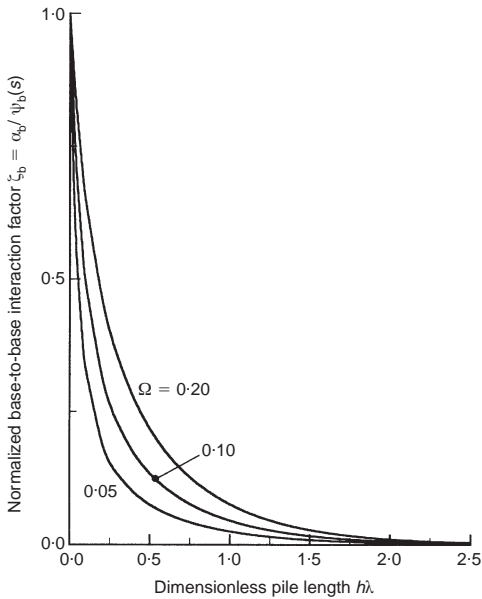


Fig. 5. Normalized base-to-base interaction factor between piles in single-layer soil (equation (18)), for different values of the dimensionless base stiffness Ω

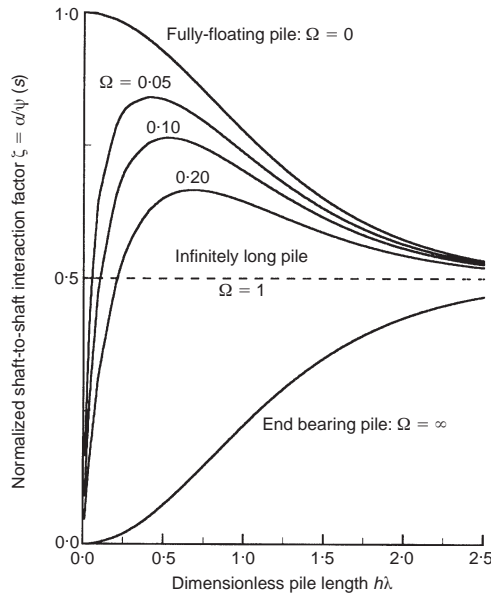


Fig. 6. Normalized shaft-to-shaft interaction factor for piles embedded in single-layer soil (equation (13)), for different values of the dimensionless base stiffness Ω

which gives

$$\zeta \equiv \frac{\alpha}{\psi(s)} = \frac{k_z h}{k_z h + K_b} \quad (19b)$$

Clearly equation (19b) gives ζ as an increasing function of h . To explain this, recall that the displacement of a *rigid* pile does not decrease with depth; hence, any increase in pile length produces an additional amount of interaction, while the restraining action of the spring at the base of the receiver pile remains constant.

For a very long and compressible pile, the 'source' settlement $W_{11}(z)$ attenuates substantially at large depths. Only an upper part of the pile undergoes large settlements (say within the first 20 pile diameters) which would affect the receiver pile. Below this depth, the remaining part of the receiver pile is acting as a restrainer to pile settlement. By increasing the length of the pile, the amount of interaction controlled by these first 20 pile diameters remains constant, while the restraining lower part becomes stiffer, thereby resulting in smaller receiver pile response.

For very long piles, the expression (13) developed here predicts an asymptotic convergence to $\zeta = 0.50$. To find out whether or not this behaviour is realistic, we examine the results obtained with

more rigorous solutions. Referring to equation (19b), it can be shown that the interaction factor between long and rigid piles (say $L/d > 50$) is essentially equal to $\psi(s)$, since $\zeta \rightarrow 1$ as $h \rightarrow \infty$. This clearly implies that the interaction factors of Poulos & Davis (1980), for a pile which is both long and rigid, are representative of the function $\psi(s)$. In the case of two piles spaced at $s = 2d$ in homogeneous soil with $\nu_s = 0.50$, for $L/d = 25, 50$ and 100 , Poulos's 'rigid-pile' interaction factors are 0.64, 0.68 and 0.74 respectively. From the ratio

$$\alpha \text{ (compressible)} / \alpha \text{ (rigid)} \approx \alpha / \psi(s) = \zeta \quad (20)$$

we then obtain for $E_p/E_s = 1000$ the values $\zeta = 0.89, 0.80$ and 0.62 . For $E_p/E_s = 100$, the corresponding interaction factors reported by El-Sharnouby & Novak (1990) are 0.43, 0.39 and 0.41 respectively, leading to ζ values of 0.67, 0.57 and 0.55. It is apparent that as the pile length increases, ζ approaches the value of 0.50—confirming the simple theory developed in this paper.

Figures 7 and 8 plot the interaction factors for compressible piles in homogeneous soil in terms of s/d . Comparison with corresponding results of Poulos & Davis (1980) shows reasonably good agreement for all values of E_p/E_s and pile slenderness ratios L/d larger than 10. For $L/d = 10$, equation (8) tends to underpredict the interaction

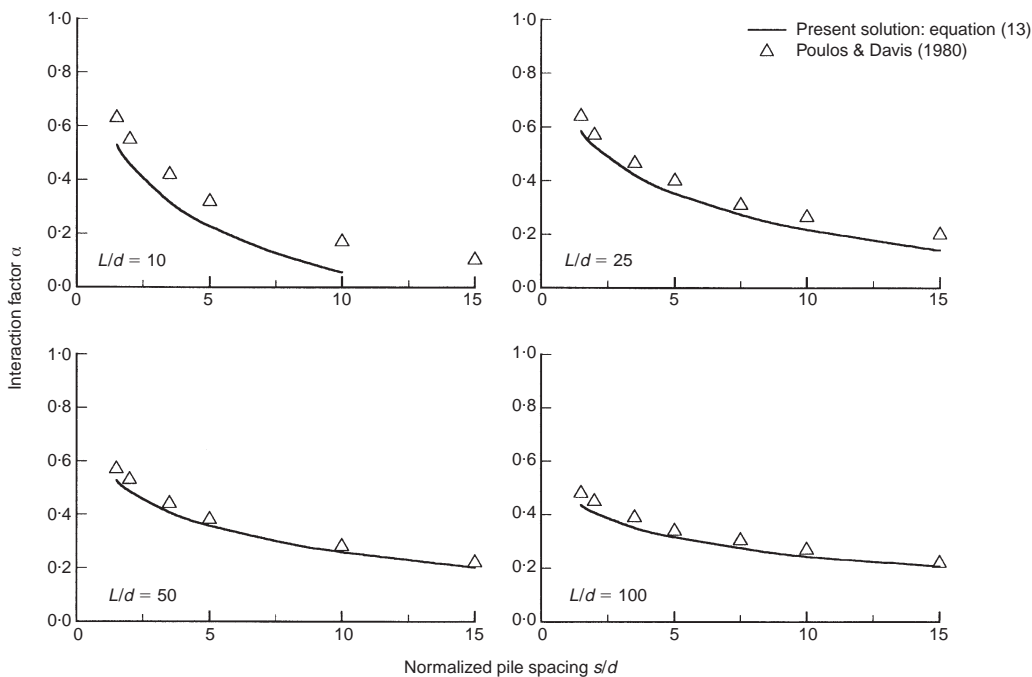


Fig. 7. Interaction factors for piles in homogeneous soil for various pile slenderness ratios L/d : comparison with Poulos & Davis (1980), $E_p/E_s = 1000$, $\nu_s = 0.50$

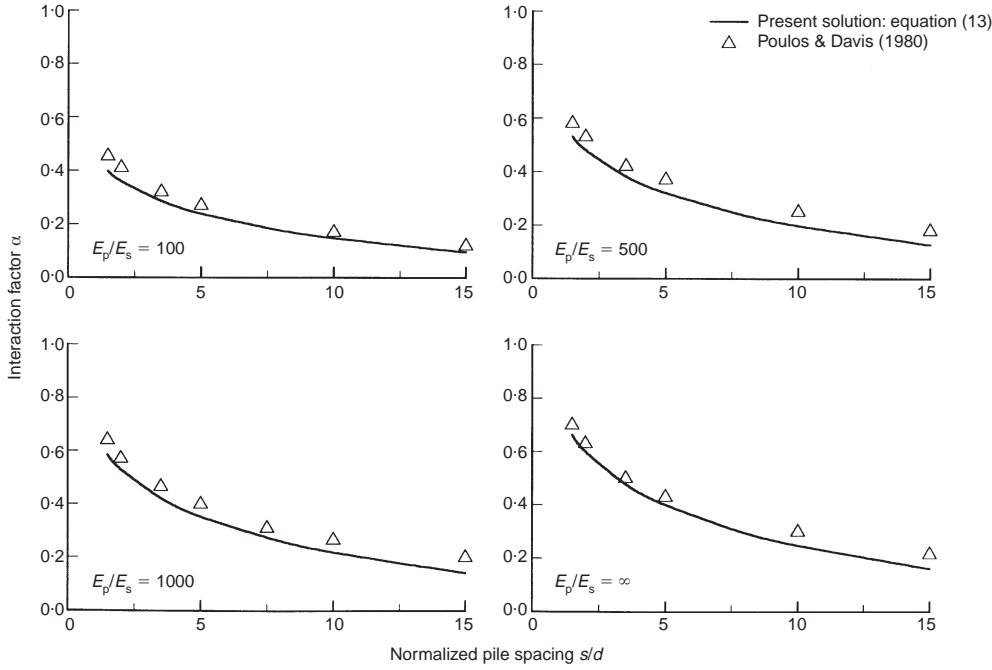


Fig. 8. Interaction factors for piles in homogeneous soil for various E_p/E_s ratios: comparison with Poulos & Davis (1980), $L/d = 25$, $\nu_s = 0.50$

values, particularly for pile spacings s/d greater than 5. This is because for such small pile lengths, the plane-strain based function $\psi(s)$ becomes gradually less effective as a predictor of the non-plane-strain pile interaction. The same deviation is observed in Randolph & Wroth (1979).

Interaction factors in layered soil

There is an inherent difficulty in deriving rigorous solutions for pile-to-pile interaction in non-homogeneous and layered soil. On one hand, finite element based analyses (which can easily treat layered soils) require substantial computational effort in three dimensions. On the other hand, there is a general lack of fundamental solutions for inhomogeneous and layered domains to support a (perhaps more suitable) boundary-element formulation. The proposed method provides a reasonably accurate and simple alternative.

To account for soil layering, equation (12) can be cast in the following transfer-matrix form:

$$\left\{ \begin{array}{l} \left\{ \begin{array}{l} W_{11}(h) \\ P_{11}(h) \end{array} \right\} \\ \left\{ \begin{array}{l} W_{21}(h) \\ P_{21}(h) \end{array} \right\} \end{array} \right\}_i = \begin{bmatrix} [L] & [0] \\ [L1] & [L] \end{bmatrix}_i \left\{ \begin{array}{l} \left\{ \begin{array}{l} W_{11}(0) \\ P_{11}(0) \end{array} \right\} \\ \left\{ \begin{array}{l} W_{21}(0) \\ P_{21}(0) \end{array} \right\} \end{array} \right\} \quad (21)$$

in which $[L]$ and $[L1]$ are 2 by 2 transfer matrices accounting for single-pile response and pile-to-pile interaction respectively. The two matrices are given in Appendix 1.

For n soil layers, applying equation (21) layer by layer, while imposing the continuity condition at each interface, leads to

$$\left\{ \begin{array}{l} W_{21} \\ P_{21} \end{array} \right\}_{bb} = \begin{bmatrix} FI_{\alpha\alpha} & FI_{\alpha\beta} \\ FI_{\beta\alpha} & FI_{\beta\beta} \end{bmatrix} \left\{ \begin{array}{l} W_{11}(0) \\ P_{11}(0) \end{array} \right\}_1 + \begin{bmatrix} F_{\alpha\alpha} & F_{\alpha\beta} \\ F_{\beta\alpha} & F_{\beta\beta} \end{bmatrix} \left\{ \begin{array}{l} W_{21}(0) \\ P_{21}(0) \end{array} \right\}_1 \quad (22)$$

in which bb denotes the base of the spring at the tip of the receiver pile. The first matrix product on the right-hand side of equation (22) is a known quantity, corresponding to the 'forcing term' produced by the source pile. Neglecting the interaction between pile bases, the settlement at the base of the spring supporting the tip of the receiver pile is zero ($W_{21bb} = 0$). Moreover, a unit settlement atop the source pile ($W_{11}(0)_1 = 1$) requires a force equal to the solitary-pile stiffness K ($P_{11}(0)_1 = K$). Then, the resulting settlement of the unloaded ($P_{21}(0)_1 = 0$) receiver pile is equal to the interaction factor α ($W_{21}(0)_1 = \alpha$). Substituting the

above boundary conditions into equation (22) the interaction factor α is readily obtained.

For instance, for the case of a two-layer soil, equation (22) gives the following closed-form expression for the interaction factor:

$$\alpha = \psi(s)\zeta(h_1\lambda_1, h_2\lambda_2, \Omega) \quad (24a)$$

where the function $\zeta = \zeta(h_1\lambda_1, h_2\lambda_2, \Omega)$ is given by

$$\begin{aligned} \zeta = & \left[\frac{2h_1\lambda_1 + \text{Sh}(2h_1\lambda_1) + \Omega_1^2[\text{Sh}(2h_1\lambda_1) - 2h_1\lambda_1] + 2\Omega_1\text{Ch}(2h_1\lambda_1) - 1}{2\text{Sh}(2h_1\lambda_1) + 2\Omega_1^2\text{Sh}(2h_1\lambda_1) + 4\Omega_1\text{Ch}(2h_1\lambda_1)} \right. \\ & + \frac{2\Omega_1}{2\Omega_1\text{Ch}(2h_1\lambda_1) + \text{Sh}(2h_1\lambda_1)(\Omega_1^2 + 1)} \\ & \left. + \frac{2h_2\lambda_2 + \text{Sh}(2h_2\lambda_2) + \Omega^2[\text{Sh}(2h_2\lambda_2) - 2h_2\lambda_2] + 2\Omega[\text{Ch}(2h_2\lambda_2) - 1]}{2\text{Sh}(2h_2\lambda_2) + 2\Omega^2\text{Sh}(2h_2\lambda_2) + 4\Omega\text{Ch}(2h_2\lambda_2)} \right] \\ & \times \frac{2\Omega_1}{2\Omega_1\text{Ch}(2h_1\lambda_1) + \text{Sh}(2h_1\lambda_1)(\Omega_1^2 + 1)} \quad (24b) \end{aligned}$$

with

$$\Omega_1 = \frac{\lambda_2 \Omega + \text{Th}(h_2\lambda_2)}{\lambda_1 \Omega + \text{Th}(h_2\lambda_2)}$$

and

$$\Omega = \frac{K_b}{E_p A_p \lambda_2} \quad (24c)$$

in which $\text{Sh}()$, $\text{Ch}()$ and $\text{Th}()$ stand for the hyperbolic functions $\sinh()$, $\cosh()$ and $\tanh()$ respectively. Note that for $h_1 = 0$, equation (24) reduces to the single-layer equation (13).

For the empirical parameters χ_1 and χ_2 it was shown earlier that the single-pile stiffness is abso-

lutely insensitive to their exact values. It can now be shown that the interaction factor α is similarly insensitive to the 'exact' value of the product $\chi_1\chi_2$ or, equivalently, of the magical radius r_m . To this end, the attenuation function $\psi(s)$ is calculated for two different r_m values, r_{mA} and r_{mB} , with the ratio r_{mA}/r_{mB} varying between 1.0 and 1.50. The results of this analysis are shown in Table 1. Apparently, despite the large discrepancy of 50% in r_m , the difference in interaction factors remains within 15%. The largest difference, 14.4%, applies to distant piles ($s/d = 10$), for which the interaction factor is already very small. For more closely spaced piles the average deviation is about 5% which is clearly negligible compared with the many uncertainties in real-life problems. Therefore, there is no need for a refined method to select 'exact' values for χ_1 and χ_2 . Simple engineering judgement based on the recommendation of Randolph & Wroth (1978, 1979) would suffice.

Parametric results for pile-to-pile interaction in a two-layer soil (equation (24)) are given in Fig. 9 (the soil profile is identical to that of Fig. 3). We notice that an increase of the stiffness of the bottom layer results in smaller interaction-factor values. However, for the range of parameters studied, the embedment ratio h_1/L is of secondary importance. Moreover, for $s/d < 5$ an increase of pile length from $L/d = 20$ to 40 results in a relatively small decrease in interaction value, while for $s/d > 10$ long piles interact much more strongly than shorter ones. Comparison with corresponding interaction factors calculated (by the authors) using the boundary-element-type method developed by Kaynia (1982) shows good agreement, particularly for the long ($L/d = 40$) piles.

Figure 10 contrasts the proposed method with results of the finite-element-based method of Chow (1987), who studied two interacting piles in layered

Table 1. Sensitivity of the interaction factor α to the selection of the empirical parameters χ_1 and χ_2

L/d	s/d	Case A		Case B		$\frac{r_{mA}}{r_{mB}}$	ψ_A	ψ_B	$\frac{\psi_A}{\psi_B} = \frac{\alpha_A}{\alpha_B}$	$\frac{\alpha_A - \alpha_B}{\alpha_A}$
		χ_1	χ_2	χ_1	χ_2					
20	2	2.5	1	2.5	0.9	1.11	0.66	0.65	1.01	1.35%
	2	2.5	1	2.5	0.8	1.25	0.66	0.64	1.03	2.95%
	2	2.5	0.75	2.5	0.5	1.5	0.63	0.59	1.07	6.83%
	4	2.5	0.9	2.5	0.75	1.2	0.48	0.45	1.05	5.2%
	6	2.5	0.9	2.5	0.75	1.2	0.38	0.35	1.09	7.91%
	10	2.5	0.9	2.5	0.75	1.2	0.25	0.21	1.17	14.4%
40	2	2.5	1	2.5	0.9	1.11	0.71	0.7	1.01	0.92%
	2	2.5	1	2.5	0.8	1.25	0.71	0.69	1.02	1.99%
	2	2.5	0.75	2.5	0.5	1.5	0.69	0.66	1.05	4.41%
	4	2.5	0.9	2.5	0.75	1.2	0.55	0.54	1.03	3.24%
	6	2.5	0.9	2.5	0.75	1.2	0.47	0.45	1.05	4.58%
	10	2.5	0.9	2.5	0.75	1.2	0.36	0.33	1.08	7.20%

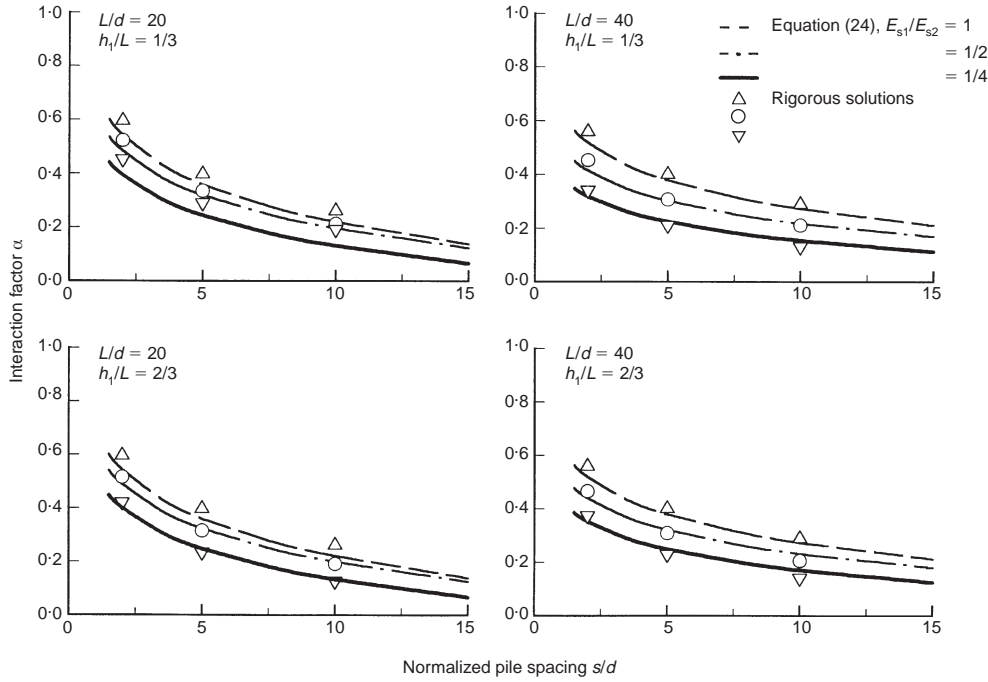


Fig. 9. Interaction factors for piles in two-layer soil (equation (24)) for various E_{s1}/E_{s2} and pile embedment ratios h_1/L : comparison with results from the rigorous solutions of Kaynia (1982) and Valliappan *et al.* (1974), $E_p/E_{s1} = 1000$, $\nu_s = 0.40$, $\chi_1 = 2.5$, $\chi_2 = 1$ for $E_{s1}/E_{s2} = 1$ and $\frac{1}{2}$, 0.75 for $E_{s1}/E_{s2} = \frac{1}{4}$

soil resting on rigid bedrock at a depth equal to two pile lengths. Four cases with different parameters (Fig. 10(a)) are studied. In cases 1 and 2 (Fig. 10(b)), a decreases very fast with pile spacing s/d . In both cases, the agreement of the two methods is very good. In contrast, the homogeneous-soil assumption grossly overestimates a . In cases 3 and 4, the agreement between the two methods is again very good. Moreover, a very interesting behaviour is observed: the stiffness of the surface layer dominates the response, leading to interaction factors very similar to those in homogeneous soil.

PILE GROUP SETTLEMENT ANALYSIS

For the usual case of a group of m identical piles on a rigid cap, one can solve for the cap settlement D_G in terms of the resultant force P_G :

$$P_G = \sum_{i=1}^m P_i = [\{1\}^T [A]^{-1} \{1\}] D_G = K_G D_G \quad (25)$$

where $[A]$ is the $m \times m$ interaction-factor matrix and $\{1\}$ is an $m \times 1$ unit vector.

The pile group efficiency (defined as the ratio of

the group stiffness to the sum of the stiffnesses of the individual piles) is shown in Table 2, for the two-layer profile of Fig. 3. The analysis refers to 2×2 and 3×3 pile groups. The agreement with the Kaynia (1982) method (results obtained by the authors) is quite satisfactory, especially for $s/d < 5$. Note that by increasing the stiffness of the bottom layer by a factor of 4, the efficiency of the group increases by about 20% for the 3×3 pile group and about 10% for the 2×2 group, compared with the corresponding homogeneous case.

ADDITIONAL INTERNAL FORCES ('DISTRESS') IN THE PILES

Interaction-factor-based methods usually design each pile as a single isolated pile carrying only its share of the cap load, determined from the group analysis. However, this is not correct because pile-to-pile interplay not only causes additional settlement at the head of each pile, but also induces shear tractions along the pile shaft.

The mechanics of this loading is illustrated in Fig. 11, showing that as the source pile settles, the displacement field developed drags the receiver pile down towards its base. This action is analogous to

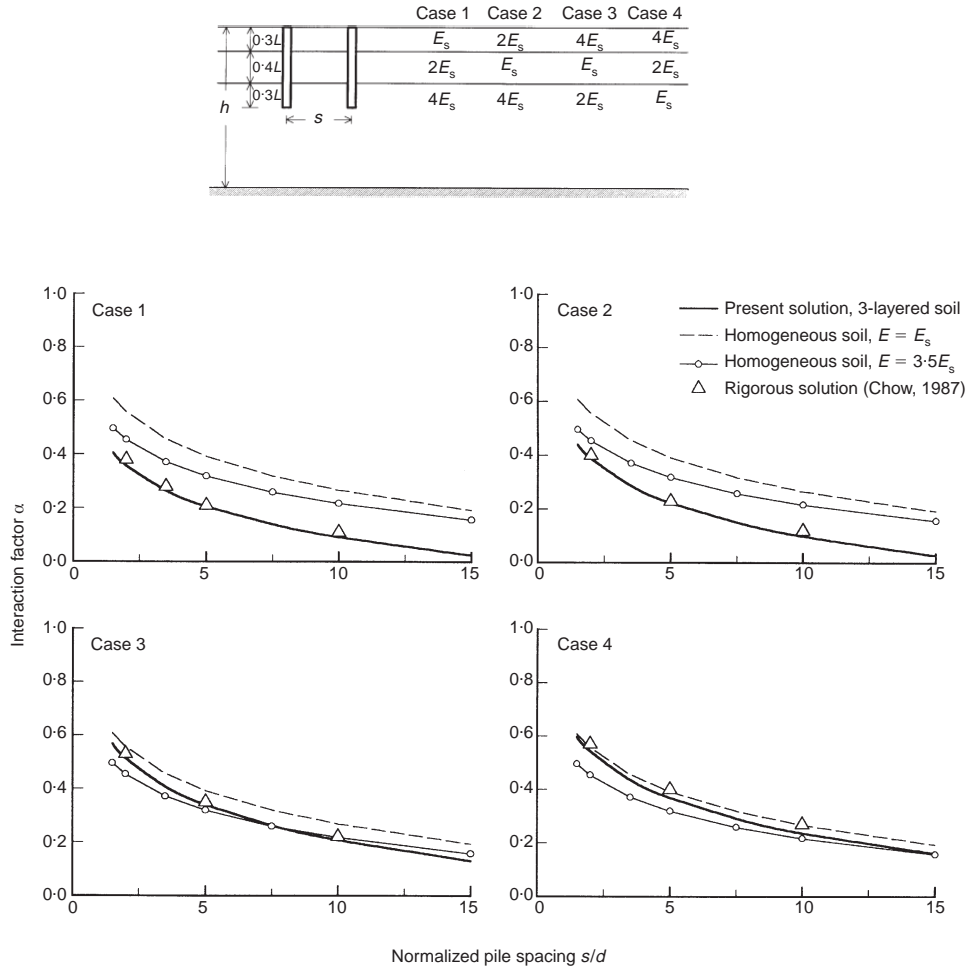


Fig. 10. Interaction factors for piles in layered soil: (a) parameters for the four cases; (b) comparison with the numerical solution of Chow (1987), for four different soil profiles resting on rigid bedrock located at $h = 2L$, $E_p/E_{s1} = 1000$, $L/d = 25$, $\nu_s = 0.30$, $\chi_1 = 2$, $\chi_2 = 0.5$ (cases 1 and 2), 0.85 (case 3) and 1 (case 4)

Table 2. Settlement efficiency factors of 2×2 and 3×3 pile groups in two-layer soil for various E_{s1}/E_{s2} ratios: comparison with results obtained by the authors using the rigorous solution of Kaynia (1982); $E_p/E_{s1} = 1000$, $L/d = 20$, $\nu_s = 0.40$, $\chi_1 = 2.5$, $\chi_2 = 1$ for $E_{s1}/E_{s2} = 1$, $\chi_2 = \frac{1}{2}$, and 0.75 for $E_{s1}/E_{s2} = \frac{1}{4}$

	s/d	Present solution			BEM		
		$E_{s1}/E_{s2} = 1$	$E_{s1}/E_{s2} = \frac{1}{2}$	$E_{s1}/E_{s2} = \frac{1}{4}$	$E_{s1}/E_{s2} = 1$	$E_{s1}/E_{s2} = \frac{1}{2}$	$E_{s1}/E_{s2} = \frac{1}{4}$
2×2	2	0.39	0.42	0.47	0.36	0.4	0.46
	5	0.5	0.52	0.52	0.47	0.54	0.6
	10	0.63	0.65	0.74	0.55	0.66	0.73
3×3	2	0.22	0.24	0.28	0.21	0.24	0.29
	5	0.32	0.34	0.42	0.29	0.35	0.43
	10	0.49	0.52	0.67	0.39	0.49	0.59

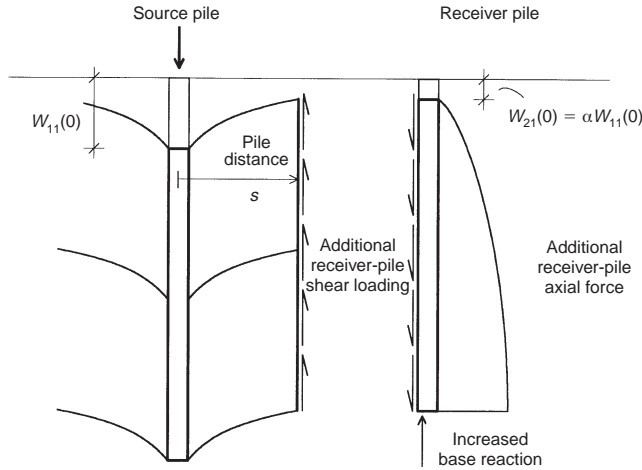


Fig. 11. Schematic illustration of the mechanism causing 'additional' loading to a receiver pile due to the displacement field of a neighbouring source pile

the 'negative friction' caused by a (downward) consolidating soil layer. The additional axial force due to these shear tractions tends to increase with depth and, combined with the head loading, leads to a more uniform axial force distribution along the pile.

Poulos (1968), among others, observed that as the number of interacting piles increases, the distribution of shear stress along the shaft changes, with larger axial stresses developing near the bottom. Ottaviani (1975) found that the load transmitted to the base of piles is much higher in the cases of 3×3 or 5×3 pile groups than for a single pile, a fact observed experimentally by O'Neil *et al.* (1982) and by Ghosh (1975). Randolph & Wroth (1979) proposed an alternative explanation for this phenomenon: the increasing proportion of the load transmitted at the base of the pile group, compared with a single pile, stems from much greater interaction between pile shafts than between the pile bases.

No simple method is presently available for computing this effect, but the analytical approach of this paper can provide an efficient method of computing 'additional' axial forces due to pile-to-pile interaction, as well as axial forces due to head loading.

Axial pile forces due to head loading

After the cap settlement D_G has been determined, the distribution of the total load among the individual piles, P_i , is obtained by inverting equation (25). Obviously, each pile carrying its own share P_i would have experienced (if alone) a settle-

ment $W_{ii} = P_i/K$, smaller than the cap settlement D_G of the group. Their difference, an additional settlement due to pile-to-pile interaction, can be written as

$$\{\delta W_i\} = \{1\}D_G - \{W_{ii}\} \quad (26)$$

in which the symbol δW denotes the additional settlement caused by the simultaneous action of all the other $m - 1$ piles in the group. The axial force and the displacement profile due to head loading can thus be easily computed along each pile i , by substituting the pair (P_i, W_{ii}) into the transfer-matrix formulation of Appendix 1.

Additional pile settlement and distress due to pile interaction

Apart from the m 'source' piles, a complementary set of m piles, governed by the 'receiving' equations (11) and (12), is conceptually introduced to compute the additional amount of settlement and distress. Having evaluated the additional head settlements δW_i (equation (26)) and knowing that the additional loading atop the receiving piles is (by definition) zero, equation (21) can produce δW_i and δP_i at any desired depth z down the pile. For example, considering the arbitrary pile i of the group, equation (21) gives

$$\begin{aligned} \begin{Bmatrix} \delta W_i(z) \\ \delta P_i(z) \end{Bmatrix} &= [L_i(z)] \begin{Bmatrix} \delta W_i \\ 0 \end{Bmatrix} \\ &+ \sum_{j=1}^{m, j \neq i} [LI(z)_{ij}] \begin{Bmatrix} W_{jj} \\ P_j \end{Bmatrix} \end{aligned} \quad (27)$$

in which the terms in the summation stand for the excitation caused by the *source* piles. Note that the symbol z has been used instead of h , to show the capability of the formulation to predict pile response at any depth z . Setting $z = h_1$, the force and displacement at the bottom of the first layer are obtained. The procedure can then be repeated for all n layers (as well as for any other pile in the group). Finally the total pile response (i.e. the total settlement and the total distress) is written as the sum of the two components, 'source' and 'received'. For pile i ,

$$\begin{Bmatrix} W_i(z) \\ P_i(z) \end{Bmatrix}_{\text{(total)}} = \begin{Bmatrix} W_{ii}(z) \\ P_i(z) \end{Bmatrix}_{\text{(source)}} + \begin{Bmatrix} \delta W_i(z) \\ \delta P_i(z) \end{Bmatrix}_{\text{(received)}} \quad (28)$$

As an example, for two piles in a homogeneous layer, substituting into equation (12) the four integration constants A_{11} , B_{11} , A_{21} and B_{21} (see Appendix 1) and differentiating with respect to z , one obtains the additional axial force along the receiver pile:

$$\begin{aligned} P_{21}(z) = & \frac{P_{11}(0)E_p A_p \lambda}{K} \left[\left(\frac{\psi}{4} - \frac{\psi K}{4E_p A_p \lambda} \right) (1 + \lambda z) e^{\lambda z} \right. \\ & - \left. \left(\frac{\psi}{4} + \frac{\psi K}{4E_p A_p \lambda} \right) (1 - \lambda z) e^{-\lambda z} \right. \\ & \left. - \left(\frac{\alpha}{2} + \frac{\psi K}{4E_p A_p \lambda} \right) e^{\lambda z} + \left(\frac{\alpha}{2} - \frac{\psi K}{4E_p A_p \lambda} \right) e^{-\lambda z} \right] \quad (29) \end{aligned}$$

in which α and K are given by equations (13) and (4a) respectively.

For infinitely long piles $K = E_p A_p \lambda$ and $\alpha = \psi/2$. Then, equation (29) simplifies to

$$P_{21}(z) = P_{11}(0) \frac{\psi}{2} \lambda z e^{-\lambda z} \quad (30)$$

Equation (30) reaches its maximum at a depth equal to $1/\lambda$, and the maximum 'received' axial force normalized to the maximum active force is

$$\frac{\max P_{21}}{P_{11}(0)} = \frac{1}{2e} \psi(s) \approx 0.18 \psi(s) \quad (31)$$

which is, remarkably, independent of the Winkler spring constant k_z .

Figure 12 depicts the axial force distribution with depth in the corner and centre piles of a

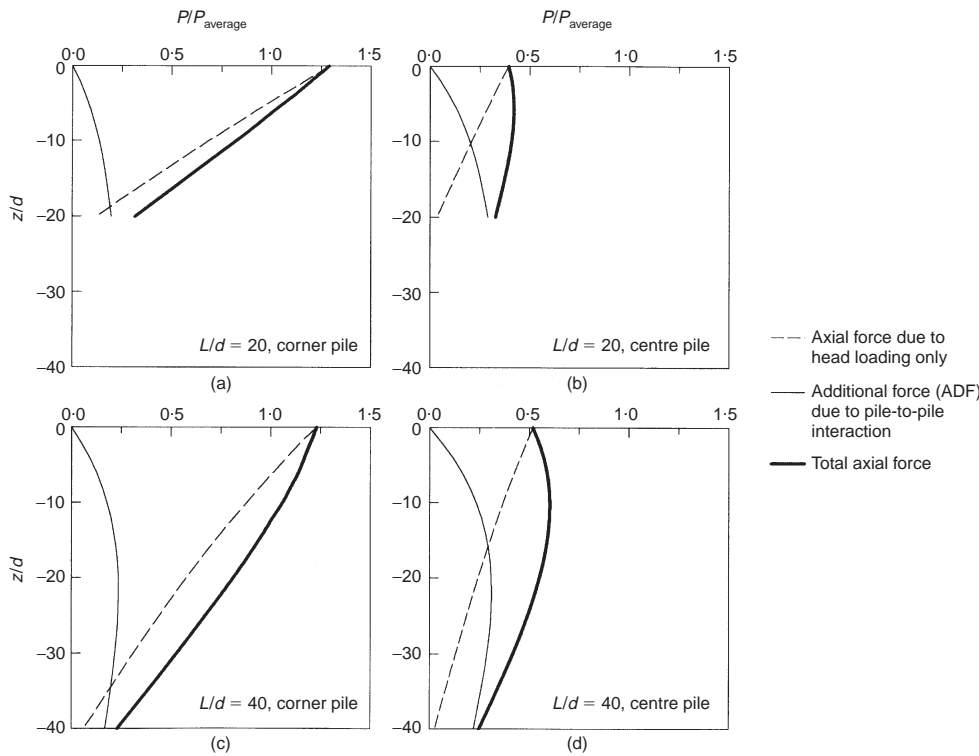


Fig. 12. Axial force distribution along the corner and centre piles of a 3×3 pile group in homogeneous soil, $E_p/E_s = 1000$, $L/d = 20$, $\nu_s = 0.40$, $s/d = 5$; notice the effect of the additional distress on piles

3×3 pile group embedded in a homogeneous soil. It is seen that for corner piles, the additional interaction force (ADF) is of secondary importance compared with the direct head loading. On the contrary, the ADF in the centre piles is a significant portion of the total axial load.

Figure 13 illustrates the sensitivity of the ADF to the specific boundary conditions at the pile tip. It appears that the stiffness of the soil 'spring' below the tip is a controlling factor in the development of additional distress. Thus, in 'fully floating' piles with no reaction at their base, the ADF is insignificant (Fig. 13(c)). An exception: for end-bearing piles (Fig. 13(d)), the undeformable support at the tip renders pile-to-pile interaction very small, thus the additional force is only 25% of the head force.

The significance of the stiffness of the soil spring is further illustrated in Fig. 13(b); the ADF was re-evaluated after reducing the spring to 80% of its initial half-space stiffness. Such a weaker base spring reduces the additional force at the tip of the passive pile by about 10%, despite the fact that it leads to an increased interaction factor.

Comparison with Ottaviani (1975)

A comparison with 3-D finite element (FE) analysis (Ottaviani, 1975) is shown graphically in Fig. 14. The plot refers to a 3×3 pile group embedded in a homogeneous soil layer, underlain by bedrock at a depth 1.5 times the pile length. The parameters of the problem are pile length $L = 40$ m, $E_p = 19\,600$ MPa, $E_s = 24.5$ MPa ($E_p/E_s = 800$), $\nu_s = 0.45$, pile spacing $s = 4$ m and square cross-section of side $a = 1$ m—compatible with the geometry of the 8-node brick elements used in the FE analysis. To make the solutions comparable, an 'equivalent' cylindrical pile is considered with the same cross-sectional area; the 'equivalent' diameter $d = 2a/\sqrt{\pi} = 1.13$ m produces a modified s/d ratio equal to about 3.50, compared to $s/a = 4$. (The alternative assumption of 'equal perimeters' would yield very similar results: $d = 1.27$ m and $s/d = 3.14$.)

The single-pile stiffness calculated by the proposed method is 407 MN/m—about 8% smaller than Ottaviani's 440 MN/m. On the other hand, the results for the group stiffness of the two methods are only approximately comparable, since Ottaviani considers a deformable concrete pile cap. Never-

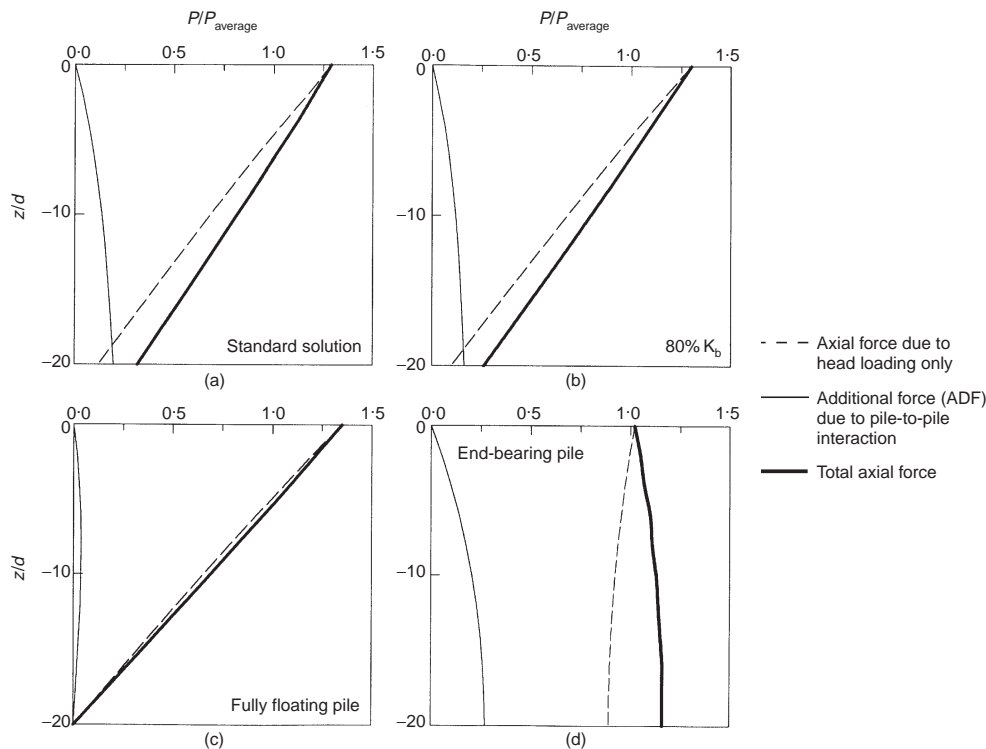


Fig. 13. Axial force distribution along the corner and centre piles of a 3×3 pile group in homogeneous soil for various boundary conditions at the pile tip, $E_p/E_s = 1000$, $L/d = 20$, $\nu_s = 0.40$, $s/d = 5$

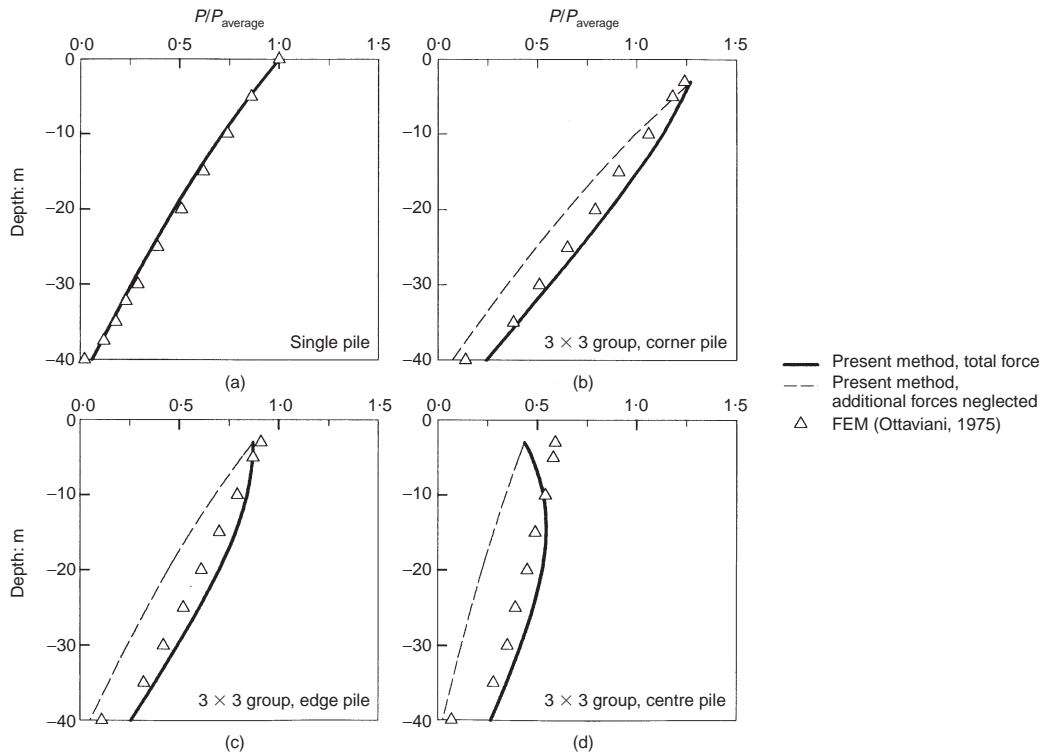


Fig. 14. Axial force distribution along (a) solitary pile; (b) corner; (c) edge; (d) centre pile of a 3×3 pile group in single-layer soil resting on rigid bedrock at $h = 1.5L$: comparison with the finite element solution of Ottaviani (1975), $E_p/E_s = 800$, $L = 40$ m for the single pile, $L = 37$ m for the group piles (cap thickness = 3 m), $d = 1$ m, $s/d = 4$, $\nu_s = 0.45$, $\chi_1 = 1.5$, $\chi_2 = 1$

theless, the agreement between the methods is satisfactory: $K_G = 1090$ MN/m and 1050 MN/m ($\eta_w = 0.30$ and 0.27) with the proposed method and the FE method respectively. The axial load is plotted against depth in Fig. 14(a) for a single pile carrying a unit load at its top. The agreement between the two approaches is very good. In Figs 14(b)–(d) the axial load is plotted against depth for the corner, edge, and centre piles of the group. Evidently, the traditional way of calculating axial forces in grouped piles, considering only the head loading, underestimates pile distress. Account of the additional axial force due to pile-to-pile interaction clearly improves the comparison with the FE solution.

Some differences, however, between the two approaches are worthy of note:

- (a) Near the tip, the FE method predicts a significant reduction in axial load, arising from a strong local concentration of shear tractions, particularly on the centre pile. The Winkler model presented does not exactly follow this

trend, overestimating the tip reaction of the (grouped) piles.

- (b) For the centre pile (Fig. 14(d)), the total axial load from the present method exhibits a trend of initially increase with depth. The same trend was observed in Fig. 13(d) but not in the FE results. This behaviour stems from the rigidity of the pile cap (considered in our simple analysis but not in the FE model): a very small force acts atop the centre pile. As a result, the relative importance of the additional force increases, causing the above effect.

CONCLUSIONS AND LIMITATIONS

A simple physical method has been presented for calculating the settlement and distress of single piles and pile groups in multilayered soil. The basis of the method is a generalized Winkler-type model for pile–soil and pile–soil–pile interaction analysis. Extensive comparisons with available nu-

merical results confirmed the (approximate) validity of the assumptions of the method. Limitations of the method stem from the simplifying assumptions of soil linearity and perfect bonding between pile and soil (which lead to an upper bound of the possible pile-to-pile interaction effect), and the adoption of the superposition 'principle' for pile groups. The latter may not be of sufficient accuracy when applied to very large pile groups, when the pile is socketed in a very stiff bearing stratum, and when strongly non-linear soil response prevails.

Nevertheless, the method developed here permits many key parameters to be evaluated through closed-form expressions and valuable insight to be gained on the mechanics of load transfer between pile and soil and on the interplay between neighbouring piles, in a multilayered soil. It is believed that the results of the paper complement and extend the seminal work on the topic by Poulos (1968, 1989) and by Randolph & Wroth (1978, 1979).

APPENDIX 1. TRANSFER MATRIX FORMULATION

For n soil layers, repeating the equation of motion, $W_{11}(z) = A_{11} \exp[\lambda z] + B_{11} \exp[-\lambda z]$, for each homogeneous layer, while imposing the continuity of forces and displacements at each interface, we take

$$\begin{Bmatrix} W_{11}(h) \\ P_{11}(h) \end{Bmatrix}_{\text{bb}} = [\mathbf{F}] \begin{Bmatrix} W_{11}(0) \\ P_{11}(0) \end{Bmatrix}_1 \quad (32a)$$

where

$$[\mathbf{F}] = [\mathbf{L}]_{\text{b}} \prod_{i=1}^j ([\mathbf{L}]_i) \quad (32b)$$

The transfer matrices $[\mathbf{L}]_{\text{b}}$ and $[\mathbf{L}]_i$ are:

$$[\mathbf{L}]_i = \begin{bmatrix} \cosh(\lambda_i h_i) & -(E_p A_p \lambda_i)^{-1} \sinh(\lambda_i h_i) \\ E_p A_p \lambda_i \sinh(\lambda_i h_i) & \cosh(\lambda_i h_i) \end{bmatrix} \quad (33)$$

$$[\mathbf{L}]_{\text{b}} = \begin{bmatrix} 1 & -K_{\text{b}}^{-1} \\ 0 & 1 \end{bmatrix} \quad (34)$$

Enforcing the boundary conditions $W_{11}(h)_{\text{bb}} = 0$ and $W_{11}(0)_1 = 1$, the stiffness of a solitary pile is easily obtained from equation (32a):

$$K = -\frac{F_{11}}{F_{12}} \quad (35)$$

Moreover, for a given force atop the pile, the pile response at the bottom of any layer j can be calculated as

$$\begin{Bmatrix} W_{11}(h) \\ P_{11}(h) \end{Bmatrix}_j = \prod_{i=1}^j ([\mathbf{L}]_i) \begin{Bmatrix} -K^{-1} \\ 1 \end{Bmatrix} P_{11}(0)_1 \quad (36)$$

For two interacting piles, the transfer matrix equation is written as (Mylonakis, 1995)

$$\begin{Bmatrix} W_{21}(h) \\ P_{21}(h) \end{Bmatrix}_i = [\mathbf{L}]_i \begin{Bmatrix} W_{11}(0) \\ P_{11}(0) \end{Bmatrix}_i + [\mathbf{L}]_i \begin{Bmatrix} W_{21}(0) \\ P_{21}(0) \end{Bmatrix}_i \quad (37)$$

in which $[\mathbf{L}]$ is given by equation (33) and $[\mathbf{L}]_i$ by

$$[\mathbf{L}]_i = (k_{z_i} + i\omega c_{z_i}) \frac{\psi(s)}{2\lambda_i} \begin{bmatrix} -\frac{h_i}{E_p A_p} \sinh(h_i \lambda_i) \\ h_i \lambda_i \cosh(h_i \lambda_i) + \sinh(h_i \lambda_i) \\ \frac{1}{(E_p A_p)^2 \lambda_i} \left[h_i \cosh(h_i \lambda_i) - \frac{\sinh(h_i \lambda_i)}{\lambda_i} \right] \\ -\frac{h_i}{E_p A_p} \sinh(h_i \lambda_i) \end{bmatrix} \quad (38)$$

The four integration constants A_{11} , B_{11} , A_{21} and B_{21} are given by

$$A_{11} = \frac{1}{2} - \frac{K}{2E_p A_p \lambda} \quad B_{11} = \frac{1}{2} + \frac{K}{2E_p A_p \lambda} \quad (39a)$$

$$A_{21} = \frac{\psi(s)}{2} \left(\zeta - \frac{K}{2E_p A_p \lambda} \right) \quad B_{21} = \frac{\psi(s)}{2} \left(\zeta + \frac{K}{2E_p A_p \lambda} \right) \quad (39b)$$

REFERENCES

- Baguelin, F. & Frank, R. (1979). Theoretical studies of piles using the finite element method. *Numerical Methods in Offshore Piling*. Institution of Civil Engineers, London, pp. 83–91.
- Banerjee, P. K. & Davies, T. G. (1978). The behaviour of axially and laterally single piles embedded in non-homogeneous soils. *Géotechnique* **28**, No. 3, 309–326.
- Butterfield, R. & Banerjee, P. K. (1971). The elastic analysis of compressible piles and pile groups. *Géotechnique* **21**, No. 1, 43–60.
- Chow, Y. K. (1986). Discrete element analysis of settlement of pile groups. *Computers & Structures* **24**, No. 1, 157–166.
- Chow, Y. K. (1987). Axial and lateral response of pile groups embedded in nonhomogeneous soils. *Int. J. Num. Anal. Meth. Geomech.* **11**, 621–638.
- Cooke, R. W. (1974). The settlement of friction pile foundations. *Proc. Conf. Tall Buildings, Kuala Lumpur*.
- Gazetas, G. (1983). Analysis of machine foundation vibration: state of the art. *Soil Dyn. Earthq. Engng* **2**, No. 1, 2–41.
- Ghosh, N. (1975). *A model scale investigation of the working load stiffness of single piles and groups of piles in clay under centric and eccentric vertical loads*. PhD thesis, University of Southampton.
- El Sharnouby, B. & Novak, M. (1990). Stiffness constants and interaction factors for vertical response of pile groups. *Can. Geotech. J.* **27**, 813–822.

- Fleming, W. G. K., Weltman, A. J., Randolph, M. F. & Elson, W. K. (1992). *Piling engineering*, 2nd edn. Wiley.
- Kausel, E. (1974). *Forced vibrations of circular foundations on layered media*. Research report R74-11, Massachusetts Institute of Technology.
- Kaynia, A. M. (1982). *Dynamic stiffness and seismic response of pile groups*. Research report R82-03, Massachusetts Institute of Technology.
- Makris, N. & Gazetas, G. (1992). Dynamic pile-soil-pile interaction. Part II: Lateral and seismic response. *Earthq. Engng & Struct. Dyn.* **21**, No. 2, 145-162.
- Mylonakis, G. (1995). *Contributions to static and seismic analysis of piles and pile-supported bridge piers*. PhD thesis, State University of New York at Buffalo.
- Nogami, T. & Chen, H. L. (1984). Simplified approach for axial pile group response analysis. *J. Geotech. Engng, ASCE* **110**, No. 9, 1239-1255.
- O'Neill, M. W., Hawkins, R. A. & Mahar, L. J. (1982). Load transfer mechanisms in piles and pile groups. *J. Geotech. Engng, ASCE* **108**, No. 12, 1605-1623.
- Ottaviani, M. (1975). Three-dimensional finite element analysis of vertically loaded pile groups. *Géotechnique* **25**, No. 2, 159-174.
- Poulos, H. G. (1968) Analysis of the settlement of pile groups. *Géotechnique* **18**, 449-471.
- Poulos, H. G. (1989). Pile behaviour—theory and application. *Géotechnique* **39**, No. 3, 365-415.
- Poulos, H. G. & Davis, E. H. (1980). *Pile foundation analysis and design*. Wiley.
- Randolph, M. F. & Wroth, C. P. (1978). Analysis of deformation of vertically loaded piles. *J. Geotech. Engng, ASCE* **104**, No. 12, 1465-1488.
- Randolph, M. F. & Wroth, C. P. (1979). Analysis of vertical deformation of pile groups. *Géotechnique* **29**, No. 4, 423-439.
- Scott, R. F. (1981). *Foundation analysis*. Prentice-Hall.
- Sokolnikoff, I. S. & Redheffer, R. M. (1966). *Mathematics of physics and modern engineering*, 2nd edn. McGraw-Hill.
- Valliappan, S., Lee, I. K. & Boonlualohr, P. (1974). Settlement of piles in layered soils. *Proc. 7th Biennial Conf. Aust. Rd. Res. Bd., Adelaide*, Vol. 7, Part 7, pp. 144-153.